

Brief Communication



Low-Dose Radiotherapy Attenuates Experimental Autoimmune Arthritis by Inducing Apoptosis of Lymphocytes and Fibroblast-Like Synoviocytes

Bo-Gyu Kim ^{1,2,†}, Hoon Sik Choi ^{3,4,†}, Yong-ho Choe ^{1,5,6}, Hyun Min Jeon ¹, Ji Yeon Heo ¹, Yun-Hong Cheon ^{1,2,7}, Ki Mun Kang ^{3,4}, Sang-il Lee ^{1,2,7}, Bae Kwon Jeong ^{4,8,*}, Mingyo Kim ^{1,2,7,*}

¹Division of Rheumatology, Department of Internal Medicine, Gyeongsang National University Hospital, Jinju 52727, Korea

²Department of Convergence Medical Science, College of Medicine, Gyeongsang National University, Jinju 52727, Korea

³Department of Radiation Oncology, Gyeongsang National University Changwon Hospital, Changwon 51472, Korea

⁴Department of Radiation Oncology and Institute of Health Science, College of Medicine, Gyeongsang National University, Jinju 52727, Korea

⁵Department of Veterinary Obstetrics, College of Veterinary Medicine, Gyeongsang National University, Jinju 52828, Korea

⁶Lillehei Heart Institute and Cardiovascular Division, Department of Medicine, University of Minnesota, Minneapolis, MN 55414, USA

⁷Department of Internal Medicine, College of Medicine, Gyeongsang National University, Jinju 52727, Korea

⁸Department of Radiation Oncology, Gyeongsang National University Hospital, Jinju 52727, Korea

OPEN ACCESS

Received: Dec 23, 2023

Revised: Jul 24, 2024

Accepted: Jul 31, 2024

Published online: Aug 12, 2024

*Correspondence to

Bae Kwon Jeong

Department of Radiation Oncology and Institute of Health Science, College of Medicine, Gyeongsang National University, 15 Jinju-daero 816beon-gil, Jinju 52727, Korea.
Email: blue129j@hanmail.net

Mingyo Kim

Division of Rheumatology, Department of Internal Medicine, Gyeongsang National University Hospital, 79 Gangnam-ro, Jinju 52727, Korea.
Email: mingyokim@gnu.ac.kr

[†]Bo-Gyu Kim and Hoon Sik Choi contributed equally to this work.

Copyright © 2024. The Korean Association of Immunologists

This is an Open Access article distributed under the terms of the Creative Commons Attribution Non-Commercial License (<https://creativecommons.org/licenses/by-nc/4.0/>) which permits unrestricted non-commercial use, distribution, and reproduction in any medium, provided the original work is properly cited.

ORCID iDs

Bo-Gyu Kim

<https://orcid.org/0000-0002-6479-4044>

Yong-ho Choe

<https://orcid.org/0000-0003-0788-4745>

<https://immunenetw.org>




ABSTRACT

Low-dose radiotherapy (LDRT) has been explored as a treatment option for various inflammatory diseases; however, its application in the context of rheumatoid arthritis (RA) is lacking. This study aimed to elucidate the mechanism underlying LDRT-based treatment for RA and standardize it. LDRT reduced the total numbers of immune cells, but increased the apoptotic CD4⁺ T and B220⁺ B cells, in the draining lymph nodes of collagen induced arthritis and K/BxN models. In addition, it significantly reduced the severity of various pathological manifestations, including bone destruction, cartilage erosion, and swelling of hind limb ankle. Post-LDRT, the proportion of apoptotic CD4⁺ T and CD19⁺ B cells increased significantly in the PBMCs derived from human patients with RA. LDRT showed a similar effect in fibroblast-like synoviocytes as well. In conclusion, we report that LDRT induces apoptosis in immune cells and fibroblast-like synoviocytes, contributing to attenuation of arthritis.

Keywords: Inflammation; Experimental arthritis; Rheumatoid arthritis; Radiotherapy; Apoptosis; Synoviocytes

INTRODUCTION

Rheumatoid arthritis (RA) is a chronic and systemic autoimmune disease characterized by joint synovial hypertrophy and excessive inflammatory response (1,2). Disease-modifying anti-rheumatic drugs (DMARDs) are a vital therapy for RA that work by regulating the

Sang-Il Lee 
<https://orcid.org/0000-0002-8283-7001>
 Bae Kwon Jeong 
<https://orcid.org/0000-0001-8015-6061>
 Mingyo Kim 
<https://orcid.org/0000-0003-3744-8522>

Conflict of Interest

The authors declare no potential conflicts of interest.

Abbreviations

Bak1, Bcl-2-antagonist/killer 1; Bax, Bcl-2-associated X protein; CIA, collagen-induced arthritis; dLN, draining lymph node; DMARD, disease-modifying anti-rheumatic drugs; FLS, fibroblast-like synoviocytes; LDRT, low-dose radiotherapy; Micro-CT, micro-computed tomography; PARP, poly ADP-ribose polymerase; qRT-PCR, real-time quantitative PCR; RA, rheumatoid arthritis.

Author Contributions

Conceptualization: Kim BG, Choi HS, Choe YH, Jeong BK, Kim M; Data curation: Kim BG, Choi HS, Choe YH, Kang KM, Lee SI; Formal analysis: Kim BG, Choe YH, Jeon HM, Heo JY, Cheon YH; Funding acquisition: Choi HS, Jeong BK, Lee SI, Kim M; Investigation: Kim BG, Choi HS, Choe YH, Jeon HM, Heo JY; Methodology: Jeon HM, Heo JY, Cheon YH, Jeong BK, Kim M; Project administration: Jeong BK, Kim M; Resources: Choi HS, Lee SI, Jeong BK, Kim M; Software: Kim BG, Choe YH, Jeon HM, Heo JY, Kim M; Supervision: Jeong BK, Kim M; Validation: Kim BG, Choi HS, Cheon YH, Kang KM; Visualization: Kim BG, Choi HS, Kang KM, Lee SI; Writing – original draft: Kim BG, Choi HS, Jeong BK, Kim M; Writing – review & editing: Jeong BK, Kim M.

immune responses. However, a substantial proportion of patients fail to attain a sufficient therapeutic response to these, while a significant number fail to sustain such a response, due to either treatment-related toxicity or a lack of therapeutic efficacy (3,4).

In a significant proportion of patients for whom DMARDs treatment proves ineffective, surgical intervention becomes imperative, to address the functional limitations. However, joint surgery as a therapeutic approach for RA also presents inherent drawbacks, including the potential for surgical site infections, substantial financial burdens, and challenges in managing the daily activities of patients and their postoperative consequences (5,6). Low-dose radiotherapy (LDRT) can be considered as one of the treatment options for patients with resistance to DMARDs treatment and an alternative to surgical intervention.

In a broad sense, LDRT means a radiation dose of ≤100 mSV or one that is lower than a conventional radiotherapy dose (7). The radiobiological effect of LDRT is different from that of the high-dose radiotherapy commonly used for malignant tumors (8). High-dose radiotherapy can induce simultaneous and irreversible DNA double-strand breaks in genes, resulting in anti-proliferative effects in cancer cells and anti-tumor immune responses through regulation of inflammation. On the other hand, LDRT induces reversible DNA damage that can be repaired and is known to have anti-inflammatory effects that reduce existing inflammation.

Several studies have reported the application of LDRT as a therapeutic modality for arthritis (9-11). More recently, LDRT has been shown to improve arthritic symptoms by inhibiting the expression of cartilage metabolic factors in chondrocytes in an osteoarthritis model (12). However, these studies primarily employed intra-articular injection or systemic inflammation models, which differ from our experimental design (13-15). In addition, there is insufficient evidence on the efficacy of LDRT in the treatment of animal models with autoimmune arthritis or patients with RA.

One of the most prominent biological effects that stems from radiation exposure is the initiation of apoptosis via intracellular pathways. Notably, LDRT has the ability to trigger apoptosis by mediating intracellular ROS signaling and the TGF-β pathway (16,17). Apoptosis is a programmed and accurate cell death process that makes up most biological cell death. Also, the apoptosis of various immune cells acts as a fundamental modulator of innate and adaptive immune responses (18). In contrast, impaired apoptosis of pathological cells such as Th1, Th17, and B cells can cause dysregulation of inflammatory cytokines and autoantigen-recognized Ab production (19). Therefore, overcoming apoptosis resistance inhibits the growth of abnormally activated immune cells, leading to the mitigation of inflammatory diseases. Meanwhile, other studies have reported upregulated apoptotic immune cells in human PBMCs exposed to low-dose radiation in a discontinuous manner (20-22). Although it is known that radiotherapy can induce apoptosis in immune cells, there is still insufficient research on the use of LDRT for treating inflammatory diseases through this mechanism. Specifically, there is a lack of research on RA treatment that can upregulate apoptosis of immune cells through LDRT, to improve joint inflammation and bone destruction.

Therefore, in this study, we explored how LDRT alleviates arthritis symptoms using two diverse autoimmunity-based arthritis models. The ultimate goal of this research was to assess the potential of LDRT as an alternative strategy that can mitigate the resistance to DMARDs treatment and overcome the limitations associated with surgical intervention.

MATERIALS AND METHODS

Procurement of PBMCs and fibroblast-like synoviocytes (FLS) from patients with RA

Human RA-PBMCs were provided by Gyeongsang National University Hospital (Jinju, Korea) a constituent of the Korea Biobank Network. Informed written consent was obtained from all patients or their families prior to participation. The disease activity of RA was assessed in terms of the Disease Activity Score-28, which incorporated both clinical and laboratory data (23). The human FLS derived from patient with RA employed in this investigation were generously supplied by Gyeongsang National University Hospital. This study received approval from the Institutional Review Board of Gyeongsang National University Hospital (permit No: GNUH-2022-07-008).

Establishment of the collagen-induced arthritis (CIA) mouse model

Male DBA/1 mice aged eight wk were purchased from The Jackson Laboratory (Yokohama, Japan) and stabilized by housing for 1 wk. The CIA model was established using stabilized 8–9-wk-old DBA/1 mice, as described previously (24). After 7 days of secondary immunization, the CIA mice were divided into two groups: 1) CIA (control) and 2) LDRT (4 Gy). All animal experiments were performed according to the guidelines of the Laboratory Animal Ethics Committee of Gyeongsang National University (permit No: GNU-211117-M0100).

Generation of the K/BxN mouse model

K/BxN mice were obtained by crossmating KRN TCR-transgenic mice with a C57BL/6 background and non-obese diabetic mice. The K/BxN mice were group-housed (up to 5 per cage) in a specific pathogen-free barrier facility (with maintained room temperature and humidity) under a 12 h/12 h dark/light cycle and fed standard diet. After housing for seven wk, the K/BxN mice were divided into two groups: 1) K/BxN (control) and 2) LDRT (2 Gy). All animal experiments were performed according to the guidelines of the Laboratory Animal Ethics Committee of Gyeongsang National University (permit No: GNU-211117-M0100).

Scoring of inflammatory arthritis and measurement of ankle thickness

The severity of arthritis was observed and the clinical scores of arthritis were assessed every 2–3 days, for 2 wk. The inflammation level of the hind paw was graded from 0 to 4, as per the following scale: 0=no swelling or redness among digits, insteps, and joints; 1=paw with swelling or redness in a single site; 2=paw with swelling or redness in two sites; 3=paw with swelling or redness in three sites; and 4=severe swelling or redness at all sites and stiffness of ankle joint. The clinical scores were measured for 2 wk and scores of the hind paws were summed. Hind paw thickness of the K/BxN mice was measured with a caliper placed across the ankle-joint (at the widest site) on the day of the sacrifice.

In vivo irradiation treatment of the animal models

Irradiation was performed at room temperature using a 6 MV photon beam from a linear accelerator (21EX; Varian, Palo Alto, CA, USA) with a 1-cm bolus. Mice were anesthetized with isoflurane before each irradiation. CIA mice received a total radiation dose of 4 Gy administered in 8 fractions of 0.5 Gy each, once every three days for two wk, followed by treatments every other day for one additional week, totaling 21 days of irradiation exposure. On the other hand, K/BxN mice were treated 4 times with 0.5 Gy per fraction, every other day, for 7 days, resulting in a total irradiation dose of 2 Gy. Irradiation was confined to the lower body below the hip joint on both sides of the mouse.

Flow cytometry analysis

The list of fluorochrome-conjugated mouse Abs utilized in flow cytometry experiments is presented in **Table 1**. The isolated splenocytes and lymphocytes were incubated with Abs, following established protocols (25), for flow cytometric analysis. Assessments were conducted using the LSRFortessa™ X-20 Cell Analyzer (657666R1; BD Biosciences, Franklin Lakes, NJ, USA). The flow cytometry data were analyzed using FlowJo software version 10 (Ashland, OR, USA).

Assessment of apoptotic cells

To determine the apoptosis levels of immune cells, isolated cells were labeled using the FITC Annexin V Apoptosis Detection Kit I (556547; BD Pharmingen, San Diego, CA, USA), according to the manufacturer’s instructions. The samples were analyzed using the BD LSRFortessa™ X-20 Cell Analyzer. The flow cytometry data were analyzed using FlowJo software version 10.

Cell proliferation assay

To assess the proliferation of immune cells, the isolated cells were stained using the Cell Trace™ CFSE Cell Proliferation Kit (C34554; Thermo Fisher Scientific, Waltham, MA, USA). CFSE-labeled immune cells were incubated in Roswell Park Memorial Institute medium supplemented with 10% fetal bovine serum, 1% penicillin-streptomycin, and anti-mouse CD3 (553057) and CD28 (553294) (both from BD Biosciences) for 3 days, at 37°C, in round-bottomed 96-well plates. The cultured cells were then analyzed using a LSRFortessa™ X-20 Cell Analyzer. The flow cytometry data were analyzed using FlowJo software version 10.

Immunoblotting

B220⁺ B and CD4⁺ T cells were sorted by negative selection using MACS columns (130-090-544; Miltenyi Biotec, Bergisch Gladbach, Germany), and lysed in radioimmunoprecipitation buffer (89901; Thermo Fisher Scientific) supplemented with protease inhibitor (535142; Calbiochem, Seoul, Korea) to enable the collection of whole protein fractions. The protein fractions obtained from B220⁺ B and CD4⁺ T cells were utilized immunoblotting assay as described previously (26). Details of the Abs utilized for immunoblotting are provided in **Table 2**.

Table 1. The information of Abs used for surface and intracellular staining

Ab	Company	Cat#
PE anti-human CD4	BioLegend	317410
BV605 anti-human CD19	BioLegend	302244
APC anti-mouse CD4	Invitrogen	17-0042-82
PE-cyanine 7 anti-mouse CD44	Invitrogen	25-0441-82
APC anti-mouse IL-17A	Invitrogen	17-7177-81
FITC anti-mouse IFN-γ	Invitrogen	11-7311-82
PE-Cy7 anti-mouse B220	BD Pharmingen	552772
BV506 Fixable Viability Dye eFlour™ 506	Invitrogen	65-0866-14

Table 2. The specific Abs employed in the immunoblotting assays

Ab	Company	Cat#
Anti-mouse Bax	Santa Cruz Biotechnology	SC-7480
Anti-mouse Bak1	Santa Cruz Biotechnology	SC-518146
Anti-mouse caspase-3	Cell Signaling Technology	9665S
Anti-mouse cleaved caspase-3	Cell Signaling Technology	9661S
Anti-mouse PARP	Cell Signaling Technology	9542S
Anti-mouse cleaved PARP	Cell Signaling Technology	9579S
Anti-mouse beta actin	Abcam	8226

Bax, Bcl-2-associated X protein; Bak1, Bcl-2-antagonist/killer 1; PARP, poly ADP-ribose polymerase.

Micro-computed tomography (micro-CT)

For micro-CT imaging analysis, the Quantum FX (PerkinElmer, Waltham, MA, USA) imaging system was used to evaluate the bone destruction in the ankle joints of the K/BxN mice hind paws. The joints were scanned at 90 kV, 180 μ A for 2 min and reconstructed into a 3-dimensional structure with a voxel size of 40 μ m. The images were analyzed using Analyze 12.0 system (bone mineral density standard curve: $3.8815 \times + 1,875.7$, threshold: 5,000). The detailed information regarding the analysis conditions, methods, and equipment utilized for micro-CT imaging can be found in **Supplementary Data 1**.

Real-time quantitative PCR (qRT-PCR)

Total RNA of B220⁺ B and CD4⁺ T cells from the draining lymph nodes (dLNs) were isolated and assayed by qRT-PCR, as described previously (24). Relative mRNA expression levels were normalized to the expression of *GAPDH*. The primers sequences used for the qRT-PCR are listed in **Table 3**.

Statistical analysis

All results have been presented as mean \pm SEM. An unpaired two-tailed Student's *t*-test was used to compare two experimental groups. For comparison of more than two groups, one-way or two-way ANOVA was used. Statistical data was analyzed using GraphPad Prism version 8.0 software (San Diego, CA, USA). Differences were considered statistically significant at $p < 0.05$.

RESULTS

LDRT induces apoptosis of dLN CD4⁺ T cells and attenuates inflammatory arthritis

We established a CIA model in DBA/1 mice, to investigate the effect of LDRT on inflammatory arthritis. After three wk of LDRT, the DBA/1 mice were sacrificed (**Fig. 1A**). The clinical scores of the hind paws were evaluated from the day of the second immunization until the day of sacrifice. Since LDRT was administered locally to the hip-joint of the DBA/1 mice, the clinical scores of the fore paws were excluded from the assessment. The mice treated with LDRT displayed significantly reduced hind paw swelling and clinical scores than the control CIA mice (**Fig. 1B and C**).

Next, we isolated immune cells from the spleen and dLNs of the CIA (control) and LDRT groups and assessed their total cell numbers. There was a significant decrease in the total cell numbers only in the dLNs of the LDRT group, but not the spleen, as compared to that in the CIA group (**Fig. 1D**). To elucidate the reason for the reduced total cell number, we evaluated the proliferation, differentiation, and apoptosis of the dLN-CD4⁺ T cells. LDRT did not affect the proliferation of dLN-CD4⁺ T cells (**Fig. 1E**). In addition, the proportions of IFN- γ and IL-17A-producing CD4⁺ T cells were not different in the CIA and LDRT groups (**Fig. 1F**). Interestingly, LDRT treatment resulted in a significant increase in the apoptotic (annexin V⁺ propidium iodide⁺) CD4⁺ T cells in the dLNs, as compared to that observed in the CIA group

Table 3. The primers sequences used for the qRT-PCR

Gene	Forward (5' to 3')	Reverse (5' to 3')
<i>Bax</i>	AGACAGGGGCCTTTTGCTAC	GCTCACAGAGGCCGCTTAA
<i>Bak1</i>	CAGCTTGCTCTCATCGGAGAT	TTACGGATGCTTGC GAAGTGG
<i>Gapdh</i>	ACAAC TTTGGTATCGTGAAGG	CTTTGACACCGCACTACCG

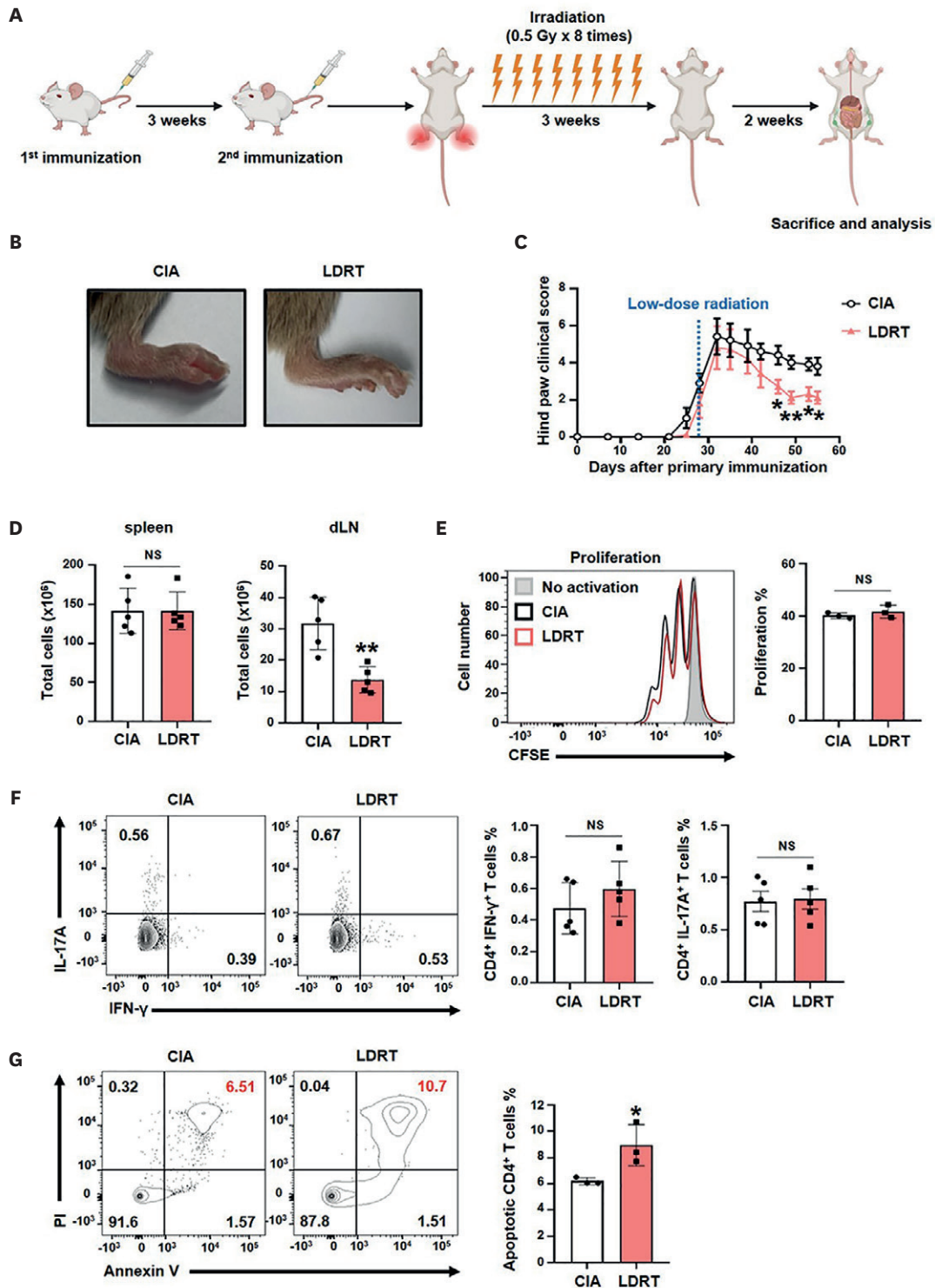


Figure 1. LDRT regulates RA incidence by inducing apoptosis of dLN-CD4⁺ T cells in CIA mice.

(A) Experimental scheme for the LDRT-treated CIA model. (B) Representative images of the hind limbs and (C) clinical scores in the CIA (n=5) and LDRT (n=5) groups. (D) The number of total immune cells were counted in the spleen and dLNs (n=5 each for the CIA and LDRT groups). (E) Comparison of CD4⁺ T cell proliferation in the CIA (n=3) and LDRT (n=3) groups. dLN cells were stained for (F) intracellular cytokines such as IL-17A or IFN- γ , at 55 days after CIA-immunization, and analyzed by means of flow cytometry (n=5 each for the CIA and LDRT groups) and (G) surface markers using propidium iodide and annexin V, to measure the level of apoptosis (n=3 each for the CIA and LDRT groups). Data are presented as mean \pm SEM. An unpaired Student's *t*-test was used to compare two groups.

NS, not significant.

p*<0.05 and *p*<0.01 vs. CIA.

(Fig. 1G). Collectively, these results demonstrate that LDRT induces apoptosis in CD4⁺ T cells in the dLN, thereby suggesting a potential therapeutic strategy for alleviating arthritis.

We then subjected the CIA model to LDRT under various conditions, to determine the optimal LDRT parameters for attenuating arthritis severity. Administering LDRT 35 days after the initial immunization, which coincided with the peak severity of arthritis, was found to be the most appropriate. In addition, the minimum LDRT dose that demonstrated a significant reduction in total immune and CD4⁺ T cell counts was determined to be 2 Gy (Supplementary Fig. 1).

LDRT attenuates the pathological manifestations in spontaneous experimental arthritis models

To prove that LDRT mitigates autoimmune-based arthritis in diverse RA models, we used a second model, a K/BxN mouse model. The K/BxN mice were treated four times (with 0.5 Gy) for two wk, at seven wk of age, when the arthritis symptoms of the mice were most severe (Fig. 2A). Similar to the results obtained in case of the CIA model, LDRT decreased the clinical score of the K/BxN mice, indicating an improvement in the arthritis symptoms (Fig. 2B). The ankle thickness of the K/BxN mice was also found to be reduced upon administration of LDRT (Fig. 2C). Furthermore, micro-CT demonstrated that LDRT attenuated the bone destruction of the hind paw (Fig. 2D). To histologically analyze if LDRT ameliorates the degree of arthritis in K/BxN mice, the hind paw tissues were stained with H&E/safranin-O after sacrifice. Subsequently, the arthritis severity score of the stained hind paw tissue was assessed using a suitable protocol for histological analysis (27). H&E staining revealed that LDRT caused a reduction in the infiltration of immune cells into the articular cavity or bone of the hind paw, as compared to that in the K/BxN mice. In addition, safranin-O staining data showed a reduction in the cartilage destruction observed in the hind paw bone of K/BxN mice upon LDRT administration (Fig. 2E and F). Moreover, LDRT significantly reduced the total number of immune and CD4⁺ T cells in the dLNs of the K/BxN mice (Fig. 2G). In congruence with findings observed in the CIA model, the diminished population of immune cells following LDRT manifested as a consequence of heightened apoptotic cells (Fig. 2H). However, flow cytometry confirmed that LDRT did not regulate the levels of proliferation (Supplementary Fig. 2A) and CD44 expression in CD4⁺ T cells (Supplementary Fig. 2B). In addition, LDRT did not affect the secretion of IFN- γ and IL-17A in CD4⁺ T cells (Supplementary Fig. 2C). These results indicated that LDRT did not inhibit the division and differentiation of Th cells, but improved the arthritis symptoms of K/BxN mice by inducing apoptosis of CD4⁺ T cells in the dLNs.

LDRT can induce the apoptosis of not only CD4⁺ T cells, but also B220⁺ B cells, in the dLNs

With the help of flow cytometry, we distinguished the total immune cells of the dLNs into three subtypes—CD4⁺ T, B220⁺ B, and B220⁻ CD4⁻ cells—to investigate whether LDRT induces apoptosis of immune cells other than CD4⁺ T cells in K/BxN mice. Interestingly, LDRT caused a significant increase in the apoptosis of B220⁺ B and CD4⁺ T cells, as compared to that observed in the K/BxN group. In contrast, LDRT did not affect the apoptosis of B220⁻ CD4⁻ cells (Fig. 3A). However, investigation into the impact of LDRT yielded no discernible alterations in the apoptotic levels of CD8⁺ T cells (Supplementary Fig. 3A and B). To verify that LDRT induces apoptosis of B220⁺ B and CD4⁺ T cells, we additionally investigated factors related to the apoptosis signaling pathway in these cells. The protein expression levels of Bcl-2-associated X protein (Bax), caspase-3, and poly ADP-ribose polymerase (PARP)

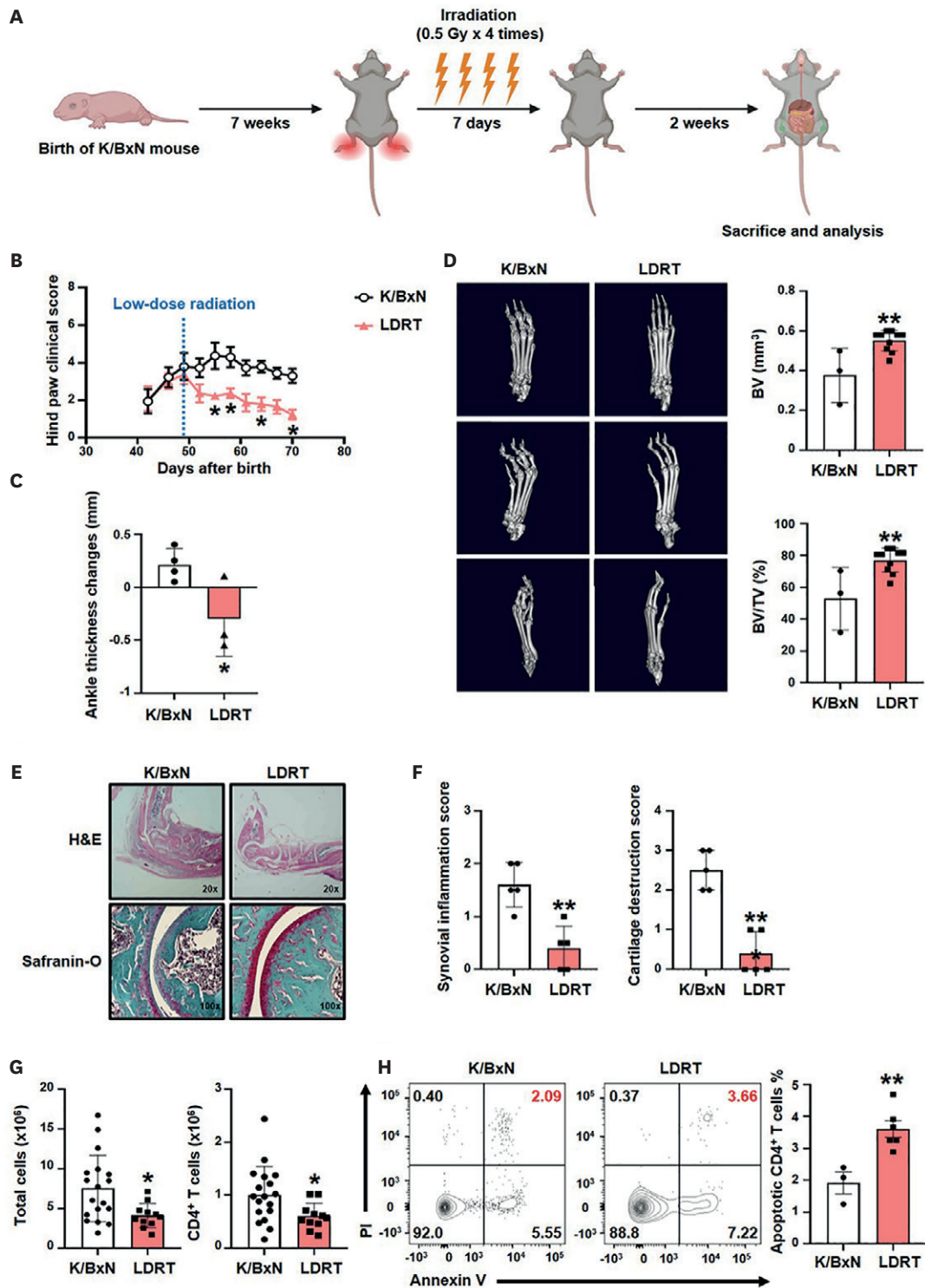


Figure 2. LDRT attenuates the pathological manifestations in a spontaneous experimental arthritis model.

(A) Experimental scheme for the LDRT-treated K/BxN model. (B) Hind limb clinical score of the K/BxN (n=7) and LDRT (n=7) groups. (C) Changes in the ankle thickness of the K/BxN (n=4) and LDRT (n=3) groups. (D) Representative micro-computed tomography images (left) of the hind paw, quantification (right) of BV and TV (n=3 for the K/BxN mice; n=10 for the LDRT group). (E) Representative images and (F) scoring of the histological staining with H&E and safranin-O in the inflamed ankle joint tissue from the K/BxN (n=5) and LDRT (n=5) groups. (G) The number of total and CD4⁺ T cells were counted in the dLNs of the K/BxN (n=18) and LDRT (n=11) groups. (H) Apoptosis levels in the CD4⁺ T cell were evaluated by staining the K/BxN (n=3) and LDRT (n=6) groups with PI and Annexin V. Data are presented as mean±SEM. An unpaired Student's *t*-test was used to compare two groups.

BV, bone volume; TV, total volume.

p*<0.05 and *p*<0.01 vs. K/BxN.

were upregulated by LDRT, and in addition, a trend of increased expression levels of Bcl-2-antagonist/killer 1 (Bak1) and cleaved PARP were observed due to LDRT in B220⁺ B cells (Fig. 3B and D). Similarly, LDRT led to an observed increase in the protein expression levels of Bax, Bak1, and cleaved PARP in CD4⁺ T cells. Further, the protein expression levels of caspase-3 and PARP were slightly upregulated by LDRT (Fig. 3C and E). We also analyzed the mRNA^{expression} levels of *Bax* and *Bak1* upon LDRT, which were prominently increased. The qRT-PCR data shows that the relative mRNA expression levels of *Bax* and *Bak1* were augmented in the LDRT group, as compared that in the K/BxN group (Fig. 3F and G). These findings indicated that LDRT contributes to the upregulation of the apoptosis signaling pathway of B220⁺ B cells, as well as CD4⁺ T cells, in dLNs.

LDRT upregulates the apoptotic cells among PBMCs and FLS obtained from patients with RA

Next, we investigated the impact of LDRT on the reduction of abnormally proliferated immune cells in patients with RA. To determine the LDRT conditions that optimally induce apoptosis in immune cells isolated from PBMCs obtained from patients with RA, we conducted a preliminary experiment that employed radiation doses of 0.5 and 2 Gy that were administered on the 3rd and 5th days following LDRT treatment. In contrast to the observation in the mouse model, preliminary *in vitro* experiments in these cells revealed the impracticability of quantifying alterations in apoptosis within PBMCs derived from patients with RA, primarily because the majority of cell deaths occurred within the 2 Gy treatment group in these cells (data not shown).

Interestingly, upon assessing cells at 3 days following 0.5 Gy treatment, flow cytometric analysis revealed that LDRT upregulated apoptosis in CD19⁺ B and CD4⁺ T cells within the PBMCs (Fig. 4A and B). In addition, we also applied LDRT to the FLS, a cell type recognized for its pivotal involvement in the onset, advancement, and inflammatory processes of RA pathogenesis, and regarded as a central contributor to joint degeneration (13,28). Surprisingly, the FLS displayed a notable increase in apoptotic cells following LDRT administration, as compared to that observed in the control group. In contrast, exposure to 0.5 Gy of LDRT did not produce a discernible effect on apoptosis in the FLS (Fig. 4C). These *in vitro* data suggested that susceptibility to induction of apoptotic cells following LDRT is not limited to CD19⁺ B and CD4⁺ T cells, but extends to FLS as well in human patients with RA.

DISCUSSION

This study provides insight into the underlying mechanism through which LDRT ameliorates arthritis symptoms in both the CIA and K/BxN models. Furthermore, in humans, LDRT was observed to elevate the levels of apoptotic CD19⁺ B, CD4⁺ T cells, and FLS derived from patients with RA. Nevertheless, the precise mechanism underlying the heightened sensitivity of B220⁺ B and CD4⁺ T cells to LDRT, as compared to that of B220⁻ CD4⁻ cells, remains unknown. Furthermore, the apoptosis of CD8⁺ T cells remained unaltered following exposure to LDRT. Additionally, it is essential to substantiate the local vs. systemic anti-inflammatory effects of LDRT through rigorous experimental validation. This can be achieved by quantifying anti-collagen Ab titers in serum and assessing collagen-specific T cells in spleen tissue. These further studies are essential to ensure both the safety and efficacy of LDRT as a treatment for patients with RA.

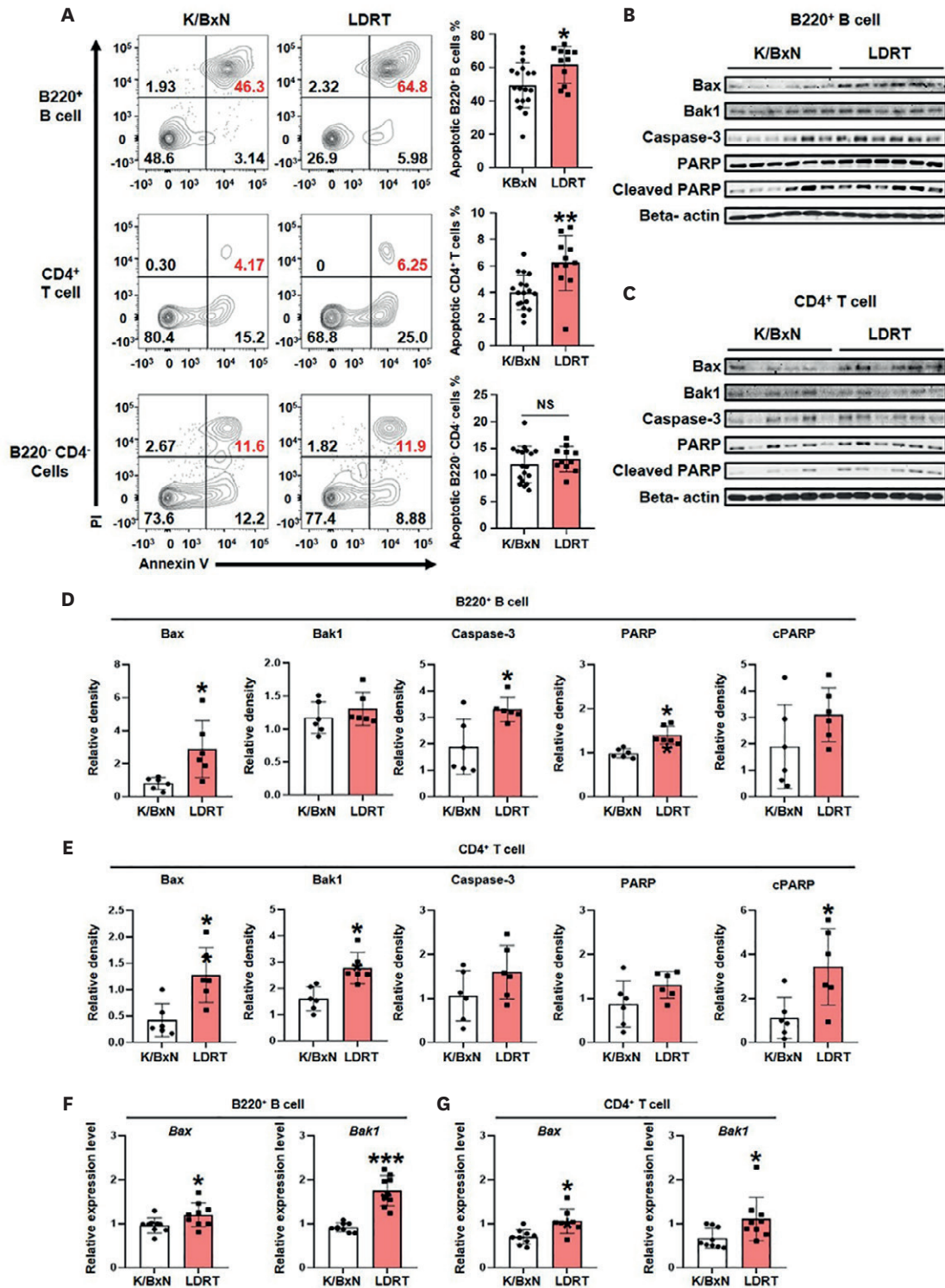


Figure 3. LDRT can induce the apoptosis of not only CD4⁺ T cells, but also B220⁺ B cells, in the dLNs.

(A) Apoptotic B220⁺ B, CD4⁺ T, and B220⁺ CD4⁻ cells in the dLNs of the K/BxN (n=18) and LDRT (n=11) groups were measured by means of flow cytometry. (B, C) The proteins involved in the apoptosis signaling pathway in the B220⁺ B (B) and CD4⁺ T (C) cells of the K/BxN (n=6) and LDRT (n=6) groups were analyzed by means of immunoblotting. (D, E) Quantification of immunoblotting in panels (B) and (C). ImageJ was used to quantify the density of band relative to the loading control, beta-actin. (F, G) Comparison of relative mRNA levels of *Bax* and *Bak1* in B220⁺ B (F) and CD4⁺ T (G) cells in the K/BxN (n=9) and LDRT (n=9) groups. Data are presented as mean±SEM. An unpaired Student's *t*-test was used to compare two groups.

NS, not significant.

p*<0.05, *p*<0.01, ****p*<0.001 vs. K/BxN.

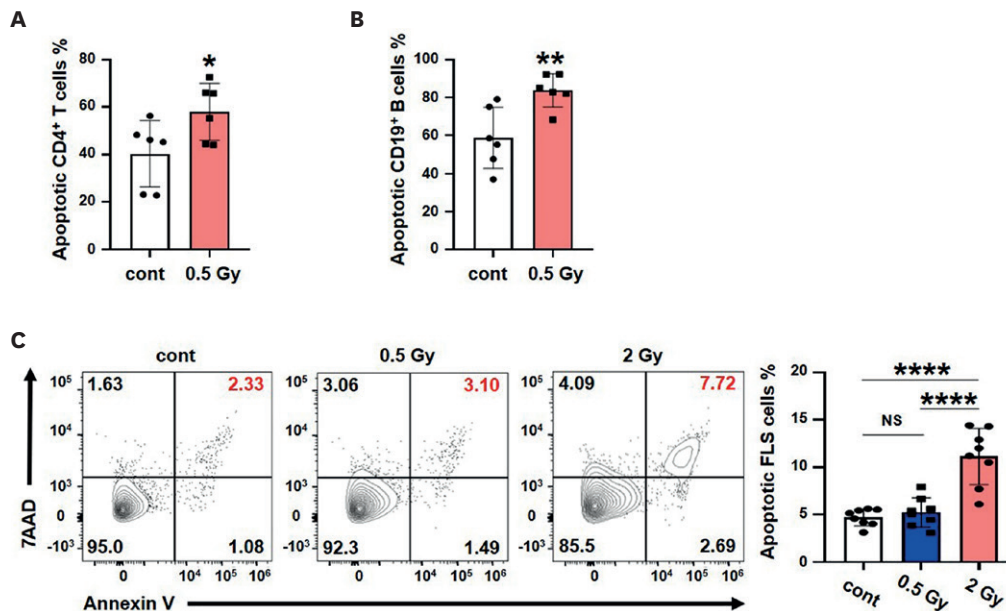


Figure 4. LDRT upregulates apoptotic cells in the PBMCs and FLS obtained from patients with RA. (A, B) Human PBMCs obtained from patients with RA were treated with 0.5 Gy irradiation, and analyzed by means of flow cytometry after three days of treatment, for assessment of the proportions of apoptotic CD4⁺ T (A) and CD19⁺ B (B) cells (n=6 patients with RA). (C) The apoptotic FLS from human patients with RA were evaluated using flow cytometry, after three days of treatment with 0.5 and 2 Gy of LDRT (n=8 patients with RA). An unpaired Student's *t*-test was used to compare two groups. 7AAD, 7-aminoactinomycin D. **p*<0.05, ***p*<0.01, *****p*<0.0001 vs. control.

Consequently, inducing apoptosis in the immune and stromal cells of patients RA through LDRT represents a hopeful therapeutic strategy. This approach addresses the limitations of current RA treatments and can potentially alleviate the pain of patients, while reducing the necessity for surgical interventions. Additionally, LDRT offers the advantage of local administration and a shorter treatment duration, as compared to that observed with the medications used for RA. Conclusively, the above advantages and our findings suggest that LDRT may emerge as a novel treatment approach, exerting distinct modulation of the immune response, unlike the mechanisms employed by existing RA therapies.

ACKNOWLEDGEMENTS

This study was supported by grants from the Basic Science Research Program through the National Research Foundation of Korea (RS-2023-00219399), and biomedical research institute fund at Gyeongsang National University Hospital (GNUHBRIF-2021-0002).

SUPPLEMENTARY MATERIALS

Supplementary Data 1

Micro-CT imaging and quantitative analysis of bone structure

Supplementary Figure 1

Comparison of changes in total cells and CD4⁺ T cells under various conditions of LDRT in CIA mice.

Supplementary Figure 2

The impact of LDRT on the proliferation, activation, and differentiation of CD4⁺ T cells was found to be negligible.

Supplementary Figure 3

Comparison of apoptotic CD4⁺ and CD8⁺ T cells in the dLNs of the K/BxN mice.

REFERENCES

1. Scherer HU, Häupl T, Burmester GR. The etiology of rheumatoid arthritis. *J Autoimmun* 2020;110:102400. [PUBMED](#) | [CROSSREF](#)
2. Wu J, Feng Z, Chen L, Li Y, Bian H, Geng J, Zheng ZH, Fu X, Pei Z, Qin Y, et al. TNF antagonist sensitizes synovial fibroblasts to ferroptotic cell death in collagen-induced arthritis mouse models. *Nat Commun* 2022;13:676. [PUBMED](#) | [CROSSREF](#)
3. Baker KF, Isaacs JD, Thompson B. “Living a normal life”: a qualitative study of patients’ views of medication withdrawal in rheumatoid arthritis. *BMC Rheumatol* 2019;3:2. [PUBMED](#) | [CROSSREF](#)
4. Zhao S, Mysler E, Moots RJ. Etanercept for the treatment of rheumatoid arthritis. *Immunotherapy* 2018;10:433-445. [PUBMED](#) | [CROSSREF](#)
5. Escalante A, Beardmore TD. Risk factors for early wound complications after orthopedic surgery for rheumatoid arthritis. *J Rheumatol* 1995;22:1844-1851. [PUBMED](#)
6. Kawakami K, Ikari K, Kawamura K, Tsukahara S, Iwamoto T, Yano K, Sakuma Y, Tokita A, Momohara S. Complications and features after joint surgery in rheumatoid arthritis patients treated with tumour necrosis factor-alpha blockers: perioperative interruption of tumour necrosis factor-alpha blockers decreases complications? *Rheumatology (Oxford)* 2010;49:341-347. [PUBMED](#) | [CROSSREF](#)
7. Rithidech KN. Health benefits of exposure to low-dose radiation. *Health Phys* 2016;110:293-295. [PUBMED](#) | [CROSSREF](#)
8. Torres Royo L, Antelo Redondo G, Árquez Pianetta M, Arenas Prat M. Low-dose radiation therapy for benign pathologies. *Rep Pract Oncol Radiother* 2020;25:250-254. [PUBMED](#) | [CROSSREF](#)
9. Budras KD, Hartung K, Münzer BM. Light and electron microscopy studies of the effect of roentgen irradiation on the synovial membrane of the inflamed knee joint. *Berl Munch Tierarztl Wochenschr* 1986;99:148-152. [PUBMED](#)
10. Fischer U, Kamprad F, Koch F, Ludewig E, Melzer R, Hildebrandt G. The effects of low-dose Co-60 irradiation on the course of aseptic arthritis in a rabbit knee joint. *Strahlenther Onkol* 1998;174:633-639. [PUBMED](#) | [CROSSREF](#)
11. Calabrese EJ, Calabrese V. Reduction of arthritic symptoms by low dose radiation therapy (LD-RT) is associated with an anti-inflammatory phenotype. *Int J Radiat Biol* 2013;89:278-286. [PUBMED](#) | [CROSSREF](#)
12. Kim BH, Bae HC, Wang SY, Jang BS, Chang JH, Chie EK, Yi HS, Kwon J, Han HS, Kim HJ. Low-dose irradiation could mitigate osteoarthritis progression via anti-inflammatory action that modulates mitochondrial function. *Radiother Oncol* 2022;170:231-241. [PUBMED](#) | [CROSSREF](#)
13. Deloch L, Derer A, Hueber AJ, Herrmann M, Schett GA, Wölfelschneider J, Hahn J, Rühle PF, Stillkrieg W, Fuchs J, et al. Low-dose radiotherapy ameliorates advanced arthritis in hTNF- α tg mice by particularly positively impacting on bone metabolism. *Front Immunol* 2018;9:1834. [PUBMED](#) | [CROSSREF](#)
14. Hildebrandt G, Radlingmayr A, Rosenthal S, Rothe R, Jahns J, Hindemith M, Rödel F, Kamprad F. Low-dose radiotherapy (LD-RT) and the modulation of iNOS expression in adjuvant-induced arthritis in rats. *Int J Radiat Biol* 2003;79:993-1001. [PUBMED](#) | [CROSSREF](#)
15. Liebmann A, Hindemith M, Jahns J, Madaj-Sterba P, Weisheit S, Kamprad F, Hildebrandt G. Low-dose X-irradiation of adjuvant-induced arthritis in rats. Efficacy of different fractionation schedules. *Strahlenther Onkol* 2004;180:165-172. [PUBMED](#) | [CROSSREF](#)
16. Bauer G. Low dose radiation and intercellular induction of apoptosis: potential implications for the control of oncogenesis. *Int J Radiat Biol* 2007;83:873-888. [PUBMED](#) | [CROSSREF](#)
17. Abdel-Aziz N, Haroun RA, Mohamed HE. Low-dose gamma radiation modulates liver and testis tissues response to acute whole body irradiation. *Dose Response* 2022;20:15593258221092365. [PUBMED](#) | [CROSSREF](#)
18. Malemud CJ, Haque A, Louis NA, Wang J. Immune response and apoptosis – introduction. *J Clin Cell Immunol* 2012;S3:e001. [CROSSREF](#)

19. Taghadosi M, Adib M, Jamshidi A, Mahmoudi M, Farhadi E. The p53 status in rheumatoid arthritis with focus on fibroblast-like synoviocytes. *Immunol Res* 2021;69:225-238. [PUBMED](#) | [CROSSREF](#)
20. Lumniczky K, Impens N, Armengol G, Candéias S, Georgakilas AG, Hornhardt S, Martin OA, Rödel F, Schae D. Low dose ionizing radiation effects on the immune system. *Environ Int* 2021;149:106212. [PUBMED](#) | [CROSSREF](#)
21. Xin Y, Zhang HB, Tang TY, Liu GH, Wang JS, Jiang G, Zhang LZ. Low-dose radiation-induced apoptosis in human leukemia K562 cells through mitochondrial pathways. *Mol Med Rep* 2014;10:1569-1575. [PUBMED](#) | [CROSSREF](#)
22. Kern P, Keilholz L, Forster C, Seegenschmiedt MH, Sauer R, Herrmann M. In vitro apoptosis in peripheral blood mononuclear cells induced by low-dose radiotherapy displays a discontinuous dose-dependence. *Int J Radiat Biol* 1999;75:995-1003. [PUBMED](#) | [CROSSREF](#)
23. van Riel PL, Renskers L. The Disease Activity Score (DAS) and the Disease Activity Score using 28 joint counts (DAS28) in the management of rheumatoid arthritis. *Clin Exp Rheumatol* 2016;34:S40-S44. [PUBMED](#)
24. Kim M, Choe Y, Lee H, Jeon MG, Park JH, Noh HS, Cheon YH, Park HJ, Park J, Shin SJ, et al. Blockade of translationally controlled tumor protein attenuated the aggressiveness of fibroblast-like synoviocytes and ameliorated collagen-induced arthritis. *Exp Mol Med* 2021;53:67-80. [PUBMED](#) | [CROSSREF](#)
25. Kim D, Kim M, Kim TW, Choe YH, Noh HS, Jeon HM, Kim H, Lee Y, Hur G, Lee KM, et al. Lymph node fibroblastic reticular cells regulate differentiation and function of CD4 T cells via CD25. *J Exp Med* 2022;219:e20200795. [PUBMED](#) | [CROSSREF](#)
26. Park HJ, Jeong OY, Chun SH, Cheon YH, Kim M, Kim S, Lee SI. Butyrate improves skin/lung fibrosis and intestinal dysbiosis in bleomycin-induced mouse models. *Int J Mol Sci* 2021;22:2765. [PUBMED](#) | [CROSSREF](#)
27. Hayer S, Vervoordeldonk MJ, Denis MC, Armaka M, Hoffmann M, Bäcklund J, Nandakumar KS, Niederreiter B, Geka C, Fischer A, et al. 'SMASH' recommendations for standardised microscopic arthritis scoring of histological sections from inflammatory arthritis animal models. *Ann Rheum Dis* 2021;80:714-726. [PUBMED](#) | [CROSSREF](#)
28. Noss EH, Brenner MB. The role and therapeutic implications of fibroblast-like synoviocytes in inflammation and cartilage erosion in rheumatoid arthritis. *Immunol Rev* 2008;223:252-270. [PUBMED](#) | [CROSSREF](#)